AGU PUBLICATIONS

Geophysical Research Letters

RESEARCH LETTER
10.1002/2017GL076883

Key Points:
- The latitude where a storm reaches peak intensity is separated into two linear parts to investigate their different contributions
- Interdecadal fluctuation of annual average tropical cyclone genesis latitude is linked to the Interdecadal Pacific Oscillation
- Long-term increase of the annual mean distance from genesis to peak intensity is likely due to increasing sea surface temperatures

Supporting Information:
- Supporting Information S1

Correspondence to:
J. Song,
songjinjie@nju.edu.cn

Citation:
Song, J., & Klotzbach, P. J. (2018). What has controlled the poleward migration of annual averaged location of tropical cyclone lifetime maximum intensity over the western North Pacific since 1961? *Geophysical Research Letters*, *45*, 1148–1156. https://doi.org/10.1002/2017GL076883

Received 16 NOV 2017
Accepted 4 JAN 2018
Accepted article online 8 JAN 2018
Published online 24 JAN 2018

What Has Controlled the Poleward Migration of Annual Averaged Location of Tropical Cyclone Lifetime Maximum Intensity Over the Western North Pacific Since 1961?

Jinjie Song[1,2,3] **and Philip J. Klotzbach**[4]

[1]Key Laboratory of Mesoscale Severe Weather, Ministry of Education, Nanjing, China, [2]School of Atmospheric Sciences, Nanjing University, Nanjing, China, [3]Joint Center for Atmospheric Radar Research, CMA/NJU, Nanjing, China, [4]Department of Atmospheric Science, Colorado State University, Fort Collins, CO, USA

Abstract The long-term tendency of the average latitude at which tropical cyclones (TCs) reach their lifetime maximum intensity (LMI) over the western North Pacific (WNP) is investigated in this study. Despite the post-1961 significant poleward shift in the annual mean LMI latitude, the migration rate is nonuniform on decadal timescales, having an insignificant trend and a significant increasing trend before and after 1980, respectively. Interdecadal fluctuations of TC genesis latitude (φ_G) as well as increases in latitudinal distance between genesis position and LMI location ($\Delta\varphi$) are both responsible for the observed LMI latitude trends. The former is linked to the Interdecadal Pacific Oscillation (IPO), which favors TCs forming in the northwestern (southeastern) quadrant of the WNP in negative (positive) IPO phases. The latter primarily results from the continuous warming of WNP sea surface temperature, which further increases the maximum potential intensity and extends the region favorable for TC development to higher latitudes.

1. Introduction

Increasing attention has been paid to long-term trends in tropical cyclone (TC) activity over the global oceans during the past few decades (Knutson et al., 2010; Walsh et al., 2016). Kossin et al. (2014) has recently proposed a new climatological TC activity indicator by computing the annual averaged latitudinal location where TCs reached their lifetime maximum intensity (LMI). They found that this metric has more consistency and less uncertainty in various storm data sources than other metrics. They also reported a global poleward migration of TC LMI latitude (φ_{LMI}) between 1982 and 2009, which was further linked to notable changes in the large-scale environment of TCs associated with tropical expansion (Kossin et al., 2014). Kossin et al. (2014) argued that the poleward shift of global TC φ_{LMI} could be regulated by both intrabasin and interbasin changes in TC activity. After quantifying different contributions, Kossin et al. (2014) further indicated that the global TC φ_{LMI} trend was dominated by the intrabasin poleward migration of LMI. However, Moon et al. (2015) found that for the Northern Hemisphere, the vast majority (92%) of the increasing φ_{LMI} tendency resulted from basin-to-basin TC frequency changes.

Despite controversy on the drivers of the global TC φ_{LMI} trend, both studies found that there was a significant poleward tendency of φ_{LMI} over the western North Pacific (WNP). This poleward migration rate of φ_{LMI} in the WNP was much larger than those found in other basins (Kossin et al., 2014; Moon et al., 2015) and was consistent with the northward shift of storm surge over the WNP after the 1980s (Oey & Chou, 2016). The northward φ_{LMI} tendency over the past several decades was reproduced by using an ensemble of numerical Coupled Model Intercomparison Project Phase 5 (CMIP5) models (Kossin et al., 2016), which also indicated a continuing poleward migration into the future following the emission projections of the representative concentration pathway 8.5 (RCP8.5).

Several papers have investigated the potential contributors to the poleward shift of WNP TC φ_{LMI}. Daloz and Camargo (2017) showed that due to a northward migration of favorable environmental conditions, TC genesis moved toward higher latitudes from 1980 to 2013, which further resulted in the northward shift of φ_{LMI}. In addition, Zhan and Wang (2017) demonstrated that the φ_{LMI} variation of weak TCs (with LMI lower than 33 m s^{-1}) was the dominant factor contributing to the poleward φ_{LMI} shift of WNP TCs since 1980.

Most φ_{LMI}-related publications have focused on the period since the early 1980s. This time span, which is only around 30 years in length, may be too short to distinguish long-term trends from interdecadal variations (Chan, 2006). Decadal oscillations, e.g., the Interdecadal Pacific Oscillation (IPO) or the Pacific Decadal Oscillation (PDO), which exert significant influence on the interdecadal variability of WNP TC activity (e.g., Lee et al., 2012; Liu & Chan, 2008; Matsuura et al., 2003; Maue, 2011; Yumoto & Matsuura, 2001), possibly modulate the fluctuation of TC φ_{LMI} over the WNP. Kossin et al. (2016) investigated φ_{LMI} variations in different best track data sets since as early as 1945 and noted that the long-term trend of φ_{LMI} was somewhat reduced when the analyzed period was extended back to the middle of the last century. This varying trend in the poleward migration rate of φ_{LMI} can be attributed to interdecadal variability of the large-scale environments influencing storm activity. For instance, Kossin et al. (2016) indicated that the warm and cool PDO phases were related to the southward and northward shifts of φ_{LMI}, respectively. However, how the PDO controls the meridional displacement of φ_{LMI} needs further investigation. In response to these questions, this study investigates changes of WNP TC φ_{LMI} as well as its contributors from 1961 to 2016. Year 1961 was chosen as the starting year for three reasons. The first is that the Television Infrared Observation Satellite began monitoring in 1960, and consequently, since that time, TCs have been continuously observed (Lee et al., 2012; Liu & Chan, 2013). The second is that reconnaissance aircrafts were frequently used to detect TC formations since 1960 (Joint Typhoon Warning Center (JTWC), 1960). The third is that four agencies, including the Joint Typhoon Warning Center (JTWC), Japan Meteorological Agency (JMA), China Meteorological Administration (CMA), and Hong Kong Observatory (HKO), provide continuous TC best track data from 1961 to present. The rest of the paper is organized as follows. Section 2 describes the data and methodology used. The decadal variation of WNP TC φ_{LMI} and its contributors are examined in section 3. The paper concludes with a summary and discussion in section 4.

2. Data and Methodology

The JTWC best track data of WNP TCs between 1961 and 2016 used in this study are from the International Best Track Archive for Climate Stewardship project (v03r10; Knapp et al., 2010), including 6-hourly storm positions and intensities. In order to reduce the uncertainty among data sources and enhance the robustness of the results, only TCs simultaneously recorded in the JTWC, JMA, CMA, and HKO data sets are considered here. The φ_{LMI} is defined as the latitude where LMI is first reached (Kossin et al., 2014, 2016). The φ_{LMI} is insensitive to the temporally evolving techniques utilized to estimate the storm absolute intensity, and it was found to be of reasonable quality when the period is extended back to the presatellite era (Kossin et al., 2016).

In this study, φ_{LMI} can be decomposed into

$$\varphi_{LMI} = \varphi_G + \Delta\varphi = \varphi_G + V_\phi \times \Delta t. \quad (1)$$

Here φ_G is the latitude of the genesis location, while $\Delta\varphi$ and Δt are the latitudinal distance and the duration between storm formation and LMI, respectively. V_φ equals the proportion of $\Delta\varphi$ to Δt, which indicates the mean latitudinal translational speed when the storm is undergoing intensification.

There are two primary methods that have been used in the past to define TC formation. One approach considers the initial position in the best track file as the storm genesis point (e.g., Lee et al., 2008; Ritchie & Holland, 1999). Due to the discrepancy in the length of the TC track from different best track data sets (Kruk et al., 2010), the reliability of φ_G is reduced by interagency heterogeneity in the first recorded TC location. The other method defines storm genesis when the TC maximum sustained wind first exceeds a threshold, such as 17 m s^{-1} (e.g., Yokoi et al., 2013) or 20 m s^{-1} (e.g., Daloz & Camargo, 2017). The reliability of φ_G relies on the quality of the estimated storm absolute intensity. There exists significant uncertainty in φ_G in the presatellite era because of problematic intensity estimating techniques.

To overcome the aforementioned shortcomings of both techniques, TC formation in this study refers to the first record that is simultaneously listed by all four agencies. Two reasons are given here to illustrate the reliability of this definition. First, prior to 1987, WNP TCs were routinely monitored by aircraft reconnaissance (Martin & Gray, 1993). Unlike the vast majority of TC intensity estimates, which were done indirectly, the central positions of storms were directly observed by aircraft radar (JTWC, 1962), which markedly improved the quality of φ_G from the presatellite best track data. Second, it is of great value to compare TC tracks from

various agencies before analysis (Chu et al., 2002). The consistency in multiple best track data sets can promote the robustness and reliability of φ_G. Kossin et al. (2016) made similar arguments for φ_{LMI}. In addition, although the operational observations of WNP TCs in the presatellite era were less frequent during the night than the day, there does not exist significant difference between daytime and nighttime φ_G or φ_{LMI} (Figure S1 in the supporting information). This means that the results in our study are not significantly influenced by the issue of detection frequency.

Monthly mean sea surface temperature (SST) data are obtained from the National Oceanic and Atmospheric Administration (NOAA) Extended Reconstructed SST V4 (Huang et al., 2014), with a horizontal resolution of 2° × 2°. Monthly mean atmospheric data are provided by the National Centers for Environmental Prediction/National Center for Atmospheric Research reanalysis over a 2.5° × 2.5° grid (Kalnay et al., 1996), which are interpolated to a 2° × 2° resolution for computing the maximum potential intensity (MPI) of TCs (Emanuel, 1988). Unlike Kossin et al. (2016) and Zhan and Wang (2017), oceanic and atmospheric fields are calculated as annual averages in this study. Annual averages of several monthly indices are also applied to discuss the relationship between φ_{LMI} and climate modes, including the Niño-3.4 SST and the PDO index provided by the NOAA's Earth System Research Laboratory Physical Sciences Division (Mantua et al., 1997; Rayner et al., 2003) and the Tripole Index for the IPO (TPI) (Henley et al., 2015).

3. Results

3.1. Nonuniform Increase of φ_{LMI} From 1961 to 2016

Figure 1a displays the annual variation of WNP TC φ_{LMI} over the period from 1961 to 2016. There exists a poleward φ_{LMI} trend of 0.24° latitude decade^{-1} (statistically significant at the 0.05 level based on an *F* test), indicating a notable northward shift of TC LMI location since 1961. Note that this rate is much smaller than that documented in previous publications (Daloz & Camargo, 2017; Kossin et al., 2014; Moon et al., 2015; Zhan & Wang, 2017), which only analyzed φ_{LMI} trends since the early 1980s. This raw trend is comparable to the 1945–2013 φ_{LMI} tendency of 0.21° latitude decade^{-1} after removing the influences of El Niño–Southern Oscillation (ENSO) and PDO found by Kossin et al. (2016). Consistent with Kossin et al. (2016), the poleward migration rate of φ_{LMI} is not uniform over the past 56 years. No significant trend in φ_{LMI} is found before 1980, with a linear trend of only 0.03° latitude decade^{-1} between 1961 and 1979. The poleward migration rate of φ_{LMI} increases markedly to 0.51° latitude decade^{-1} from 1980 to 2016, which is significant at the 0.01 level based on an *F* test. This rate is similar to what was found in Zhan and Wang (2017).

To investigate the interdecadal behavior of φ_{LMI} in detail, the full study period is divided into three subperiods (1961–1977, 1978–1997, and 1998–2016) based on the filtered TPI, which identifies different IPO phases (Figure 1a). In the first two subperiods (1961–1997), the average φ_{LMI} are similar (19.6°N and 19.7°N for 1961–1977 and 1978–1997, respectively) despite being in opposite IPO phases, which further leads to an insignificant φ_{LMI} tendency during these 37 years (0.06° latitude decade^{-1}). In contrast, the mean φ_{LMI} increases to 20.7°N during the last subperiod (1998–2016), which represents a marked difference from the averaged φ_{LMI} in the previous negative IPO phase (1961–1977). Note that our result is different from Kossin et al. (2016), which linked the decadal behavior of φ_{LMI} to the PDO (IPO). Kossin et al. (2016) indicated that the cool (warm) PDO phase was related to northward (southward) φ_{LMI} migration. However, the correlation between the filtered TPI and φ_{LMI} is −0.09, which is not significant at the 0.05 level based on a Student's *t* test. To explain this difference, the relationship between φ_{LMI} and several indices are discussed below in detail. During the period from 1961 to 2016, significant correlations are found between φ_{LMI} and the Niño-3.4 SST (−0.35), the PDO index (−0.20), and the unfiltered TPI (−0.35), which indicates that the φ_{LMI} change is notably influenced by ENSO and PDO (IPO) variability on interannual timescales. Nonetheless, the insignificant relationship between φ_{LMI} and the filtered TPI means that there is not a strong relationship between φ_{LMI} and PDO (IPO) on decadal timescales. This is further confirmed by the results of the cross-spectrum analysis (Figure S2), which estimates significant correlations between φ_{LMI} and the Niño-3.4 SST, the PDO index, and the unfiltered TPI only at periods of around 5 years. Besides obtaining differing relationships based on different timescales investigated, another reason for differences in results between Kossin et al. (2016) and our study may be due to different data sources used and time periods investigated. The φ_{LMI} from TCs simultaneously recorded by all four agencies is considered here, which is slightly different from all the TCs analyzed in Kossin et al. (2016). In addition, the annual averaged TPI is applied to describe the PDO (IPO) phenomenon,

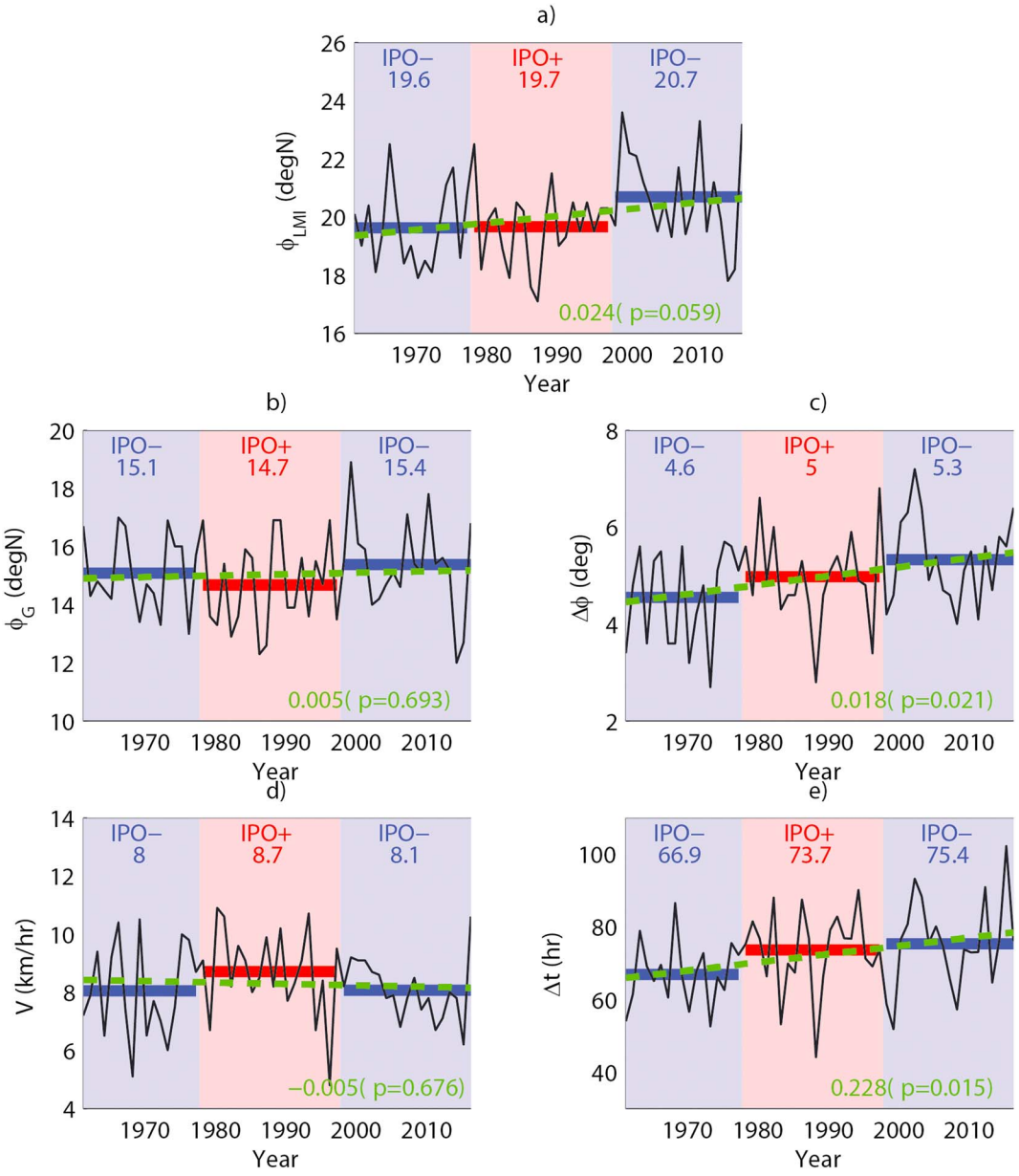

Figure 1. Time series (black solid lines) of annual mean (a) φ_{LMI}, (b) φ_G, (c) $\Delta\varphi$, (d) V_φ, and (e) Δt of TCs over the WNP from 1961 to 2016. The horizontal red and blue solid lines refer to the averages in positive and negative IPO phases, respectively. Linear trends are displayed with green dashed lines. The rate of the linear trend and confidence level are displayed in the bottom right of each panel.

compared with the seasonal (July–November) averaged PDO index from NOAA's Earth System Research Laboratory Physical Sciences Division (Mantua et al., 1997) used by Kossin et al. (2016). In the following sections, we examine interdecadal variations of φ_G and $\Delta\varphi$, since the φ_{LMI} is simply the linear combination of these two quantities.

3.2. Interdecadal Fluctuation of φ_G

Figure 1b represents the annual variation of WNP TC φ_G from 1961 to 2016. We find that the φ_G tends to be at lower latitudes in a positive IPO phase than in a negative IPO phase. The φ_G averaged 14.7°N from 1978 to 1997, which is 0.4° and 0.7° lower than the φ_G averaged from 1961 to 1977 and 1998 to 2016, respectively. The anomalies of TC genesis frequency density in different IPO phases are further illustrated in Figures 2a–2c.

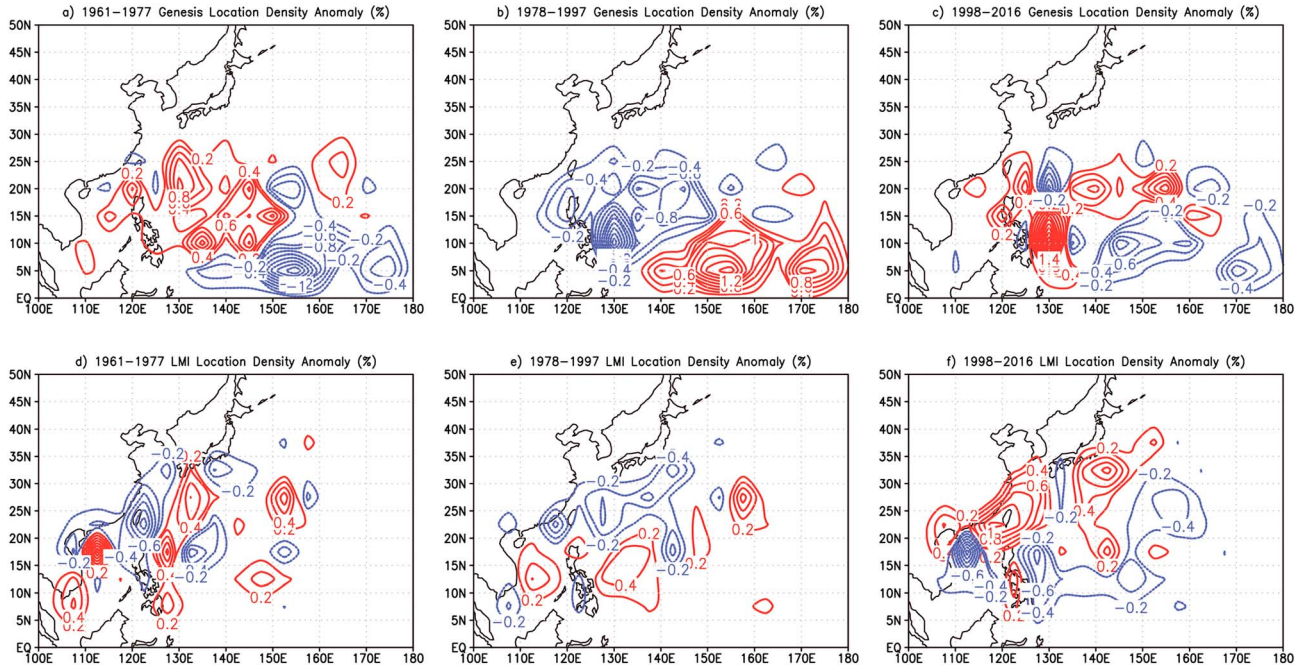

Figure 2. Density anomalies (unit: %) of (a–c) TC genesis location and (d–f) TC LMI position over a 5° × 5° grid in different IPO phases, including 1961–1977 (Figures 2a and 2d), 1978–1997 (Figures 2b and 2e), and 1998–2016 (Figures 2c and 2f). The red and blue contours represent positive and negative anomalies, respectively.

In general, TCs form more northwest (southeast) in the negative (positive) IPO phase. The primary reason is related to the interaction between the IPO and the El Niño–Southern Oscillation (ENSO). More La Niña (El Niño) events occur in the negative (positive) IPO phase (Newman et al., 2016), which tends to induce more TC occurrences in the northwestern (southeastern) quadrant of the WNP (Camargo et al., 2007; Chan, 2000). In addition, after removing the influence of ENSO, there are ENSO-like spatial signatures between different IPO phases not only in the SST field (Zhang et al., 1997) but also in the atmospheric circulation (Aiyyer & Thorncroft, 2011), which further support the observed northwest-southeast shift of TC formation (Liu & Chan, 2013).

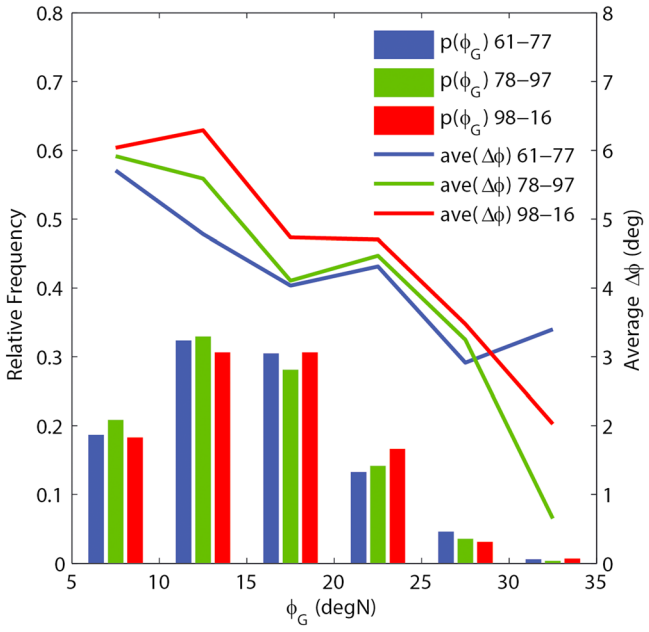

Figure 3. Relative frequencies (bars) and averages of $\Delta\varphi$ (lines) for storms forming in each 5° latitudinal band during different IPO phases. The blue, green, and red indicate the periods of 1961–1977, 1978–1997, and 1998–2016, respectively.

Due to the shift of TC genesis location in different IPO phases, the linear trend in φ_G from 1961 to 2016 is insignificant, with a rate of 0.05° latitude decade^{-1} (Figure 1b). This rate is much less than the rate of φ_G indicated by Daloz and Camargo (2017), who considered the shorter period of 1980–2013. We find that an interdecadal oscillation fits the φ_G variation better than a linear trend does. There was a general decrease in φ_G from the 1960s to the 1980s and a general increase since that time.

The inconsistency between features of φ_{LMI} and φ_G is represented in both the temporal variation (Figures 1a and 1b) as well as in the spatial distribution (Figure 2). The migration of LMI location should be greatly influenced by the shift of genesis position, with the premise being that a storm forming further north reaches its LMI at a higher latitude (Daloz & Camargo, 2017). With the shift of genesis position, the LMI location should on average migrate to the northwest (southeast) in the negative (positive) IPO phases, which can be confirmed in the last two IPO phases (1978–2016; Figures 2e and 2f). This statement does not hold true during 1961–1977, however, as there is no clear latitudinal separation between positive and negative LMI location density anomalies (Figure 2d). This implies that the movement of LMI location is not solely determined by the change in genesis position.

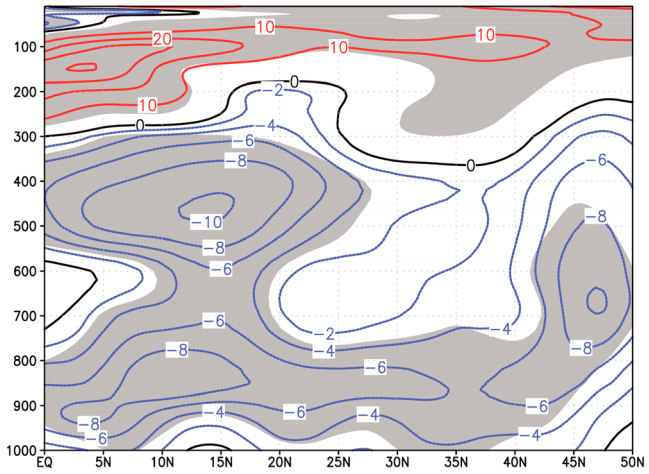

Figure 4. Linear trend ($\times 10^{-2}$ m s^{-1} decade^{-1}) of the meridional wind averaged between 100°E and 180° for 1961–2016. Positive and negative tendencies are represented by red and blue lines, respectively. Trends significant at the 0.05 level based on the *F* test are shaded.

3.3. Long-Term Uniform Increase of $\Delta\varphi$

Unlike the interdecadal fluctuation of φ_G, there is a long-term increasing trend of $\Delta\varphi$ of 0.18° latitude decade^{-1} between 1961 and 2016, which is significant at the 0.05 level based on an *F* test (Figure 1c). The averages of $\Delta\varphi$ are 4.6°, 5.0°, and 5.3° in 1961–1977, 1977–1997, and 1998–2016, respectively. Figure 3 further shows the differences of mean $\Delta\varphi$ categorized by the φ_G into each 5° latitudinal band during the three subperiods, in order to remove the influence of the genesis frequency difference. In general, $\Delta\varphi$ tends to decrease with increasing φ_G. The observed $\Delta\varphi$ increase occurs in almost all latitudinal bands from the first subperiod to the last one, except in the 30°N–35°N belt, which has a relatively small number of observed TC formations (Figure 3). This means that the increase of $\Delta\varphi$ occurs for TCs forming in various latitudinal bins in the WNP.

The $\Delta\varphi$ increase impacts φ_{LMI} variations in several different ways. First, the fact that the φ_{LMI} in the latter negative IPO phase (1998–2016) is much larger than that in the former negative IPO phase (1961–1977) is predominately a result of the upward trend in $\Delta\varphi$. Second, the increasing tendency of $\Delta\varphi$ is balanced by the decreasing trend of φ_G before 1980, which results in an insignificant trend in φ_{LMI}. By contrast, the significant poleward shift of φ_{LMI} since the early 1980s is attributed to upward trends in both φ_G and $\Delta\varphi$. Furthermore, the long-term variation of $\Delta\varphi$ dominates that of φ_{LMI} over the period of 1961–2016, explaining 75% (0.18° latitude decade^{-1}/0.24° latitude decade^{-1}) of the φ_{LMI} linear trend.

To evaluate what caused the change of $\Delta\varphi$, the variations of V_φ and Δt from 1961 to 2016 are presented in Figures 1d and 1e. There is a slight decreasing trend of V_φ during 1961–2016, with a rate of −0.05 km h^{-1} decade^{-1} (Figure 1d). Note that the tendency of $\Delta\varphi$ is opposite to that of V_φ, which means that the former is not positively correlated with the latter. Figure 4 displays the linear trend of annual mean meridional winds averaged between 100°E and 180° from 1961 to 2016. The weakened northerlies and southerlies are separated at around 300 hPa, respectively. There is a significant downward tendency of southerlies from the surface to 300 hPa in the tropical WNP (0–30°N), with two maxima at around 450 hPa and 850 hPa (Figure 4). Over the subtropical WNP (30°N–45°N), decreasing southerlies are found at lower levels (Figure 4). Through averaging meridional winds from 925 hPa to 300 hPa (Wu et al., 2003; Yang et al., 2008), the northward steering flow of WNP TCs decreases at a rate of −0.15 km h^{-1} decade^{-1}, which is larger than the downward trend of V_φ but has the same sign. Since the motion of a TC is primarily determined by its surrounding environmental flow (Holland, 1983; Roy & Kovordanyi, 2012), the decrease of $\Delta\varphi$ is largely modulated by the decelerating northward steering current over the WNP. Moreover, the decreasing environmental flow can be linked to the intensification of the Northern Hemisphere Hadley cell (Liu et al., 2012; Mitas & Clement, 2005; Nguyen et al., 2013) and the attenuation of the East Asian summer monsoon (Tanaka et al., 2004; Yu et al., 2004; Zhou et al., 2009), which can lead to both northerly (southerly) wind anomalies at lower (upper) levels.

The means of Δt are 66.9 h, 73.7 h, and 75.4 h in 1961–1977, 1977–1997, and 1998–2016, respectively (Figure 1f). This indicates an increasing trend of Δt between 1961 and 2016, with a value of 2.3 h decade^{-1} (statistically significant at the 0.05 level based on *F* test). This trend is consistent with the increasing lifetime of WNP TCs in recent decades (Emanuel, 2007; Webster et al., 2005; Wu et al., 2008). Because the Δt refers to the time span between genesis and LMI, this represents the duration of TC intensification. Figure 5 shows the 1961–2016 trend of the TC maximum potential intensity (MPI) (Bister & Emanuel, 1998; Emanuel, 1988) over the WNP. In the western region of the WNP (west of 150°E), there are significant increasing trends in MPI ranging from −1.1 hPa decade^{-1} to −2.4 hPa decade^{-1} (Figure 5a) and 0.6 m/s decade^{-1} to 1.0 m/s decade^{-1} (Figure 5b), which is consistent with the continuous warming of the tropical WNP SST during the last century (Cravatte et al., 2009; Deser et al., 2010). The region favorable for TC development and intensification has therefore been enlarged from 1961 to 2016, which means that storms can undergo intensification over a longer time period. Hart and Evans (2001) applied the 960 hPa MPI contour as the northern boundary at which purely tropical development is no longer possible. From 1961–1977 to 1998–2016, the 960 hPa MPI

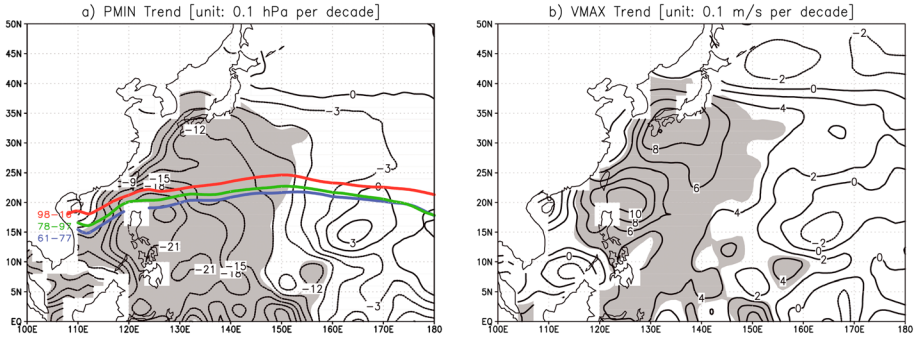

Figure 5. Linear trends for annual averages of the monthly MPI calculated from oceanic and atmospheric fields between 1961 and 2016. (a and b) The MPI trends in terms of minimum sea level pressure and maximum sustained wind, respectively. Areas with tendencies significant at the 0.05 level based on the *F* test are shaded. In Figure 5a, the blue, green, and red lines denote the 960 hPa MPI contours in 1961–1977, 1978–1997, and 1998–2016, respectively.

contour shifted approximately 3° northward (Figure 5a). This poleward migration of the 960 hPa MPI contour confirms the extended area for TC intensification. The extended region for TC intensification that is induced by the WNP SST warming first allows more time for the TC to reach its LMI, then causes the increasing latitudinal distance between the TC genesis position and LMI location, and finally contributes to the poleward shift of φ_{LMI}.

4. Summary and Discussion

In this study, long-term tendencies of WNP TC φ_{LMI} and its components (φ_G, $\Delta\varphi$, V_φ, and Δt) are examined from 1961 to 2016. Although there is a notable poleward shift of annual mean φ_{LMI} since 1961, the poleward migration rate is much smaller than those studies examining trends since ~1980 (Daloz & Camargo, 2017; Kossin et al., 2014; Moon et al., 2015; Zhan & Wang, 2017). These differences in results occur due to there being little trend in φ_{LMI} prior to 1980. The nonuniform increase of φ_{LMI} is jointly influenced by interdecadal fluctuation of φ_G and a persistent increase of $\Delta\varphi$ during 1961–2016. The effect of the upward $\Delta\varphi$ on the φ_{LMI} change before 1980 is counteracted by the decreasing φ_G due to the IPO phase shifting from negative to positive. In contrast, the poleward migration rate of φ_{LMI} is amplified over the most recent three decades when the IPO phase changes from positive to negative, due to the increasing trends in both φ_G and $\Delta\varphi$. Moreover, the increasing $\Delta\varphi$ between 1961 and 2016 is caused by a continuous increase of Δt, which measures the duration of storm intensification. Because of the steady warming of WNP SST during the past few decades, the region favorable for TC development has been enlarged, and its northern boundary is shifting poleward. Consequently, WNP TCs are more likely to begin weakening at higher latitudes, which further leads to their LMI location shifting poleward.

Kossin et al. (2016) documented a predicted continued poleward migration of WNP TC φ_{LMI} due to continued anthropogenic forcing throughout the 21st century. Given the contribution of $\Delta\varphi$ to φ_{LMI} identified in this study, one possible primary reason is the continued extension of the distance between storm genesis point and LMI position over the next several decades, which is primarily linked to SST warming and the increase of MPI over the WNP predicted by both phase 3 of the Coupled Model Intercomparison Project (CMIP3) as well as CMIP5 (Camargo, 2013; Emanuel, 2013; Wu et al., 2014). In addition, Kossin et al. (2016) represented a reduced poleward migration of φ_{LMI} in the 21th-century RCP8.5 projection, for WNP TCs both explicitly generated within the CMIP5 models and downscaled from CMIP5 model output. We further argue that this slowdown in the poleward migration rate of φ_{LMI} may result from a projected transition to a positive IPO phase in the immediate future (Meehl et al., 2016; Thoma et al., 2015).

Acknowledgments
This work was jointly funded by the National Grand Fundamental Research 973 Program of China (2015CB452800) and the National Science Foundation of China (grant 41575054). Klotzbach would like to acknowledge financial support from the G. Unger Vetlesen Foundation. We would like to express our sincere thanks to two anonymous reviewers for their helpful comments on an earlier manuscript. The data used in this study are listed in the references and at https://www.ncdc.noaa.gov/ibtracs.

References

Aiyyer, A., & Thorncroft, C. (2011). Interannual-to-multidecadal variability of vertical shear and tropical cyclone activity. *Journal of Climate*, *24*(12), 2949–2962. https://doi.org/10.1175/2010JCLI3698.1

Bister, M., & Emanuel, K. A. (1998). Dissipative heating and hurricane intensity. *Meteorology and Atmospheric Physics*, *65*(3-4), 233–240. https://doi.org/10.1007/BF01030791

Camargo, S. J. (2013). Global and regional aspects of tropical cyclone activity in the CMIP5 models. *Journal of Climate*, *26*(24), 9880–9902. https://doi.org/10.1175/JCLI-D-12-00549.1

Camargo, S. J., Emanuel, K. A., & Sobel, A. H. (2007). Use of a genesis potential index to diagnose ENSO effects on tropical cyclone genesis. *Journal of Climate*, *20*(19), 4819–4834. https://doi.org/10.1175/JCLI4282.1

Chan, J. C. L. (2000). Tropical cyclone activity over the western North Pacific associated with El Niño and La Niña events. *Journal of Climate*, *13*(16), 2960–2972. https://doi.org/10.1175/1520-0442(2000)013%3C2960:TCAOTW%3E2.0.CO;2

Chan, J. C. L. (2006). Comment on "Changes in tropical cyclone number, duration, and intensity in a warming environment". *Science*, *311*, 1713–1713.

Chu, J. -H., Sampson, C. R., Levin, A. S., & Fukada, E. (2002). The Joint Typhoon Warning Center Tropical Cyclone Best Tracks 1945–2000, Joint Typhoon Warning Center Rep., Joint Typhoon Warning Center, Pearl Harbor, HI.

Cravatte, S., Delcoix, T., Zhang, D., McPhaden, M., & LeLoup, J. (2009). Observed freshening and warming of the western Pacific warm pool. *Climate Dynamics*, *33*(4), 565–589. https://doi.org/10.1007/s00382-009-0526-7

Daloz, A. S., & Camargo, S. J. (2017). Is the poleward migration of tropical cyclone maximum intensity associated with a poleward migration of tropical cyclone genesis? *Climate Dynamics*, 1–11. https://doi.org/10.1007/s00382-017-3636-7

Deser, C., Phillips, A., & Alexander, M. (2010). Twentieth-century tropical sea surface temperature trends revisted. *Geophysical Research Letters*, *37*, L10701. https://doi.org/10.1029/2010GL043321

Emanuel, K. A. (1988). The maximum intensity of hurricanes. *Journal of the Atmospheric Sciences*, *45*(7), 1143–1155. https://doi.org/10.1175/1520-0469(1988)045%3C1143:TMIOH%3E2.0.CO;2

Emanuel, K. A. (2007). Environmental factors affecting tropical cyclone power dissipation. *Journal of Climate*, *20*(22), 5497–5509. https://doi.org/10.1175/2007JCLI1571.1

Emanuel, K. A. (2013). Downscaling CMIP5 climate models shows increased tropical cyclone activity over the 21st century. *Proceedings of the National Academy of Sciences of the United States of America*, *110*, 12, 219–12, 224.

Hart, R. E., & Evans, J. L. (2001). A climatology of extratropical transition of Atlantic tropical cyclones. *Journal of Climate*, *14*(4), 546–564. https://doi.org/10.1175/1520-0442(2001)014%3C0546:ACOTET%3E2.0.CO;2

Henley, B. J., Gergis, J., Karoly, D. J., Power, S. B., Kennedy, J., & Folland, C. K. (2015). A tripole index for the interdecadal Pacific oscillation. *Climate Dynamics*, *45*(11-12), 3077–3090. https://doi.org/10.1007/s00382-015-2525-1

Holland, G. J. (1983). Tropical cyclone motion: Environmental interaction plus a beta effect. *Journal of the Atmospheric Sciences*, *40*(2), 328–342. https://doi.org/10.1175/1520-0469(1983)040%3C0328:TCMEIP%3E2.0.CO;2

Huang, B., Banzon, V. F., Freeman, E., Lawrimore, J., Liu, W., Peterson, T. C., … Zhang, H.-M. (2014). Extended Reconstructed Sea Surface Temperature version 4 (ERSST.v4): Part I. Upgrades and intercomparisons. *Journal of Climate*, *28*, 911–930.

JTWC (1960). Annual typhoon report, Joint Typhoon Warning Center (226 pp.).

JTWC (1962). Annual typhoon report,. Joint Typhoon Warning Center (306 pp.).

Kalnay, E., Kanamitsu, M., Kistler, R., Collins, W., Deaven, D., Gandin, L., … Joseph, D. (1996). The NCEP/NCAR 40-Year Reanalysis Project. *Bulletin of the American Meteorological Society*, *77*(3), 437–471. https://doi.org/10.1175/1520-0477(1996)077%3C0437:TNYRP%3E2.0.CO;2

Knapp, K. R., Kruk, M. C., Levinson, D. H., Diamond, H. J., & Neumann, C. J. (2010). The International Best Track Archive for Climate Stewardship (IBTrACS) unifying tropical cyclone data. *Bulletin of the American Meteorological Society*, *91*(3), 363–376. https://doi.org/10.1175/2009BAMS2755.1

Knutson, T. R., McBride, J. L., Chan, J., Emanuel, K., Holland, G., Landsea, C., & Sugi, M. (2010). Tropical cyclones and climate change. *Nature Geoscience*, *3*(3), 157–163. https://doi.org/10.1038/ngeo779

Kossin, J. P., Emanuel, K. A., & Camargo, S. J. (2016). Past and projected changes in western North Pacific tropical cyclone exposure. *Journal of Climate*, *29*(16), 5725–5739. https://doi.org/10.1175/JCLI-D-16-0076.1

Kossin, J. P., Emanuel, K. A., & Vecchi, G. A. (2014). The poleward migration of the location of tropical cyclone maximum intensity. *Nature*, *509*(7500), 349–352. https://doi.org/10.1038/nature13278

Kruk, M. C., Knapp, K. R., & Levinson, D. H. (2010). A technique for combining global tropical cyclone best track data. *Journal of Atmospheric and Oceanic Technology*, *27*(4), 680–692. https://doi.org/10.1175/2009JTECHA1267.1

Lee, C.-S., Cheung, K. K. W., Hui, J. S. N., & Elsberry, R. L. (2008). Mesoscale features associated with tropical cyclone formations in the western North Pacific. *Monthly Weather Review*, *136*(6), 2006–2022. https://doi.org/10.1175/2007MWR2267.1

Lee, H. S., Yamashita, T., & Mishima, T. (2012). Multi-decadal variations of ENSO, the Pacific Decadal Oscillation and tropical cyclones in the western North Pacific. *Progress in Oceanography*, *85*, 67–80.

Liu, J., Song, M., Hu, Y., & Ren, X. (2012). Changes in the strength and width of the Hadley Circulation since 1871. *Climate of the Past*, *8*(4), 1169–1175. https://doi.org/10.5194/cp-8-1169-2012

Liu, K. S., & Chan, J. C. L. (2008). Interdecadal variability of western North Pacific tropical cyclone tracks. *Journal of Climate*, *21*(17), 4464–4476. https://doi.org/10.1175/2008JCLI2207.1

Liu, K. S., & Chan, J. C. L. (2013). Inactive period of western North Pacific tropical cyclone activity in 1998–2011. *Journal of Climate*, *26*(8), 2614–2630. https://doi.org/10.1175/JCLI-D-12-00053.1

Mantua, N. J., Hare, S. R., Zhang, Y., Wallace, J. M., & Francis, R. C. (1997). A Pacific interdecadal climate oscillation with impacts on salmon production. *Bulletin of the American Meteorological Society*, *78*(6), 1069–1079. https://doi.org/10.1175/1520-0477(1997)078%3C1069:APICOW%3E2.0.CO;2

Martin, J. D., & Gray, W. M. (1993). Tropical cyclone observation and forecasting with and without aircraft reconnaissance. *Weather Forecasting*, *8*(4), 519–532. https://doi.org/10.1175/1520-0434(1993)008%3C0519:TCOAFW%3E2.0.CO;2

Matsuura, T., Yumoto, M., & Iizuka, S. (2003). A mechanism of interdecadal variability of tropical cyclone activity over the western North Pacific. *Climate Dynamics*, *21*(2), 105–117. https://doi.org/10.1007/s00382-003-0327-3

Maue, R. N. (2011). Recent historically low global tropical cyclone activity. *Geophysical Research Letters*, *38*, L14803. https://doi.org/10.1029/2011GL047711

Meehl, G., Hu, A., & Teng, H. (2016). Initialized decadal prediction for transition to positive phase of the Interdecadal Pacific Oscillation. *Nature Communications*, *7*, 11718. https://doi.org/10.1038/ncomms11718

Mitas, C. M., & Clement, A. (2005). Has the Hadley cell been strengthening in recent decades? *Geophysical Research Letters*, *32*, L03809. https://doi.org/10.1029/2004GL021765

Moon, I.-J., Kim, S.-H., Klotzbach, P., & Chan, J. C. L. (2015). Roles of interbasin frequency changes in the poleward shifts of the maximum intensity location of tropical cyclones. *Environmental Research Letters*, *10*(10), 104004. https://doi.org/10.1088/1748-9326/10/10/104004

Newman, M., Alexander, M. A., Ault, T. R., Cobb, K. M., Deser, C., Di Lorenzo, E., … Smith, C. A. (2016). The Pacific decadal oscillation, revisited. *Journal of Climate*, *29*(12), 4399–4427. https://doi.org/10.1175/JCLI-D-15-0508.1

Nguyen, H., Evans, A., Lucas, C., Smith, I., & Timbal, B. (2013). The Hadley circulation in reanalyses: Climatology, variability, and change. *Journal of Climate*, *26*(10), 3357–3376. https://doi.org/10.1175/JCLI-D-12-00224.1

Oey, L.-Y., & Chou, S. (2016). Evidence of rising and poleward shift of storm surge in western North Pacific in recent decades. *Journal of Geophysical Research: Oceans*, *121*, 5181–5192. https://doi.org/10.1002/2016JC011777

Rayner, N. A., Parker, D. E., Horton, E. B., Folland, C. K., Alexander, L. V., Rowell, D. P., … Kaplan, A. (2003). Global analyses of sea surface temperature, sea ice, and night marine air temperature since the late nineteenth century. *Journal of Geophysical: Research*, *108*(D14), 4407. https://doi.org/10.1029/2002JD002670

Ritchie, E. A., & Holland, G. J. (1999). Large-scale patterns associated with tropical cyclogenesis in the western Pacific. *Monthly Weather Review*, *127*(9), 2027–2043. https://doi.org/10.1175/1520-0493(1999)127%3C2027:LSPAWT%3E2.0.CO;2

Roy, C., & Kovordanyi, R. (2012). Tropical cyclone track forecasting techniques—A review. *Atmospheric Research*, *104–105*, 40–69.

Tanaka, H. L., Ishizaki, N., & Kitoh, A. (2004). Trend and interannual variability of Walker, monsoon and Hadley circulations defined by velocity potential in the upper troposphere. *Tellus*, *56A*, 250–269.

Thoma, M., Greatbatch, R. J., Kadow, C., & Gerdes, R. (2015). Decadal hindcasts initialized using observed surface wind stress: Evaluation and prediction out to 2024. *Geophysical Research Letters*, *42*, 6454–6461. https://doi.org/10.1002/2015GL064833

Walsh, K. J., McBride, J. L., Klotzbach, P. J., Balachandran, S., Camargo, S. J., Holland, G., … Sugi, M. (2016). Tropical cyclones and climate change. *Wiley Interdisciplinary Reviews: Climate Change*, *7*, 65–89.

Webster, P. J., Holland, G. J., Curry, J. A., & Chang, H.-R. (2005). Changes in tropical cyclone number, duration, and intensity in a warming environment. *Science*, *309*(5742), 1844–1846. https://doi.org/10.1126/science.1116448

Wu, C.-C., Huang, T.-S., Huang, W.-P., & Chou, K. -H. (2003). A new look at the binary interaction: Potential vorticity diagnosis of the unusual southward movement of Tropical Storm Bopha (2000) and its interaction with Supertyphoon Saomai (2000). *Monthly Weather Review*, *131*(7), 1289–1300. https://doi.org/10.1175/1520-0493(2003)131%3C1289:ANLATB%3E2.0.CO;2

Wu, L., Chou, C., Chen, C.-T., Huang, R., Knutson, T. R., … Feng, Y.-C. (2014). Simulations of the present and late-twenty-first-century western North Pacific tropical cyclone activity using a regional model. *Journal of Climate*, *27*(9), 3405–3424. https://doi.org/10.1175/JCLI-D-12-00830.1

Wu, L., Wang, B., & Braun, S. A. (2008). Implications of tropical cyclone power dissipation index. *International Journal of Climatology*, *28*(6), 727–731. https://doi.org/10.1002/joc.1573

Yang, C.-C., Wu, C.-C., Chou, K.-H., & Lee, C.-Y. (2008). Binary interaction between Typhoons Fengshen (2002) and Fungwong (2002) based on the potential vorticity diagnosis. *Monthly Weather Review*, *136*(12), 4593–4611. https://doi.org/10.1175/2008MWR2496.1

Yokoi, S., Takayabu, Y. N., & Murakami, H. (2013). Attribution of projected future changes in tropical cyclone passage frequency over the western North Pacific. *Journal of Climate*, *26*(12), 4096–4111. https://doi.org/10.1175/JCLI-D-12-00218.1

Yu, R. C., Wang, B., & Zhou, T. J. (2004). Tropospheric cooling and summer monsoon weakening trend over East Asia. *Geophysical Research Letters*, *31*, L22212. https://doi.org/10.1029/2004GL021270

Yumoto, M., & Matsuura, T. (2001). Interdecadal variability of tropical cyclone activity in the western North Pacific. *Journal of the Meteorological Society of Japan*, *79*(1), 23–35. https://doi.org/10.2151/jmsj.79.23

Zhan, R., & Wang, Y. (2017). Weak tropical cyclones dominate the poleward migration of the annual mean location of lifetime maximum intensity of Northwest Pacific tropical cyclones since 1980. *Journal of Climate*, *30*(17), 6873–6882. https://doi.org/10.1175/JCLI-D-17-0019.1

Zhang, Y., Wallace, J. M., & Battisti, D. S. (1997). ENSO-like interdecadal variability: 1900–93. *Journal of Climate*, *10*(5), 1004–1020. https://doi.org/10.1175/1520-0442(1997)010%3C1004:ELIV%3E2.0.CO;2

Zhou, T., Gong, D., Li, J., & Li, B. (2009). Detecting and understanding the multi-decadal variability of the East Asian summer monsoon—Recent progress and state of affairs. *Meteorologische Zeitschrift*, *18*(4), 455–467. https://doi.org/10.1127/0941-2948/2009/0396